Preprints (www.preprints.org) | NOT PEER-REVIEWED | Posted: 10 October 2017 doi:10.20944/preprints201710.0057.v1

Peer-reviewed version available at *Materials* **2017**, *10*, 1368; doi:10.3390/ma10121368

Article

Ceramic-Based 4D-Components: Additive Manufacturing (AM) of Ceramic-Based Functionally Graded Materials (FGM) by Thermoplastic 3D-Printing (T3DP)

Uwe Scheithauer [1,*], Steven Weingarten [1], Robert Johne [2], Eric Schwarzer [1], Johannes Abel [1], Hans-Jürgen Richter [1], Tassilo Moritz [1] and Alexander Michaelis [1]

[1] Fraunhofer Institute for Ceramic Technologies and Systems, Dresden, Germany; www.ikts.fraunhofer.de
[2] Fraunhofer Singapore, Singapore; www.fraunhofer.sg
* Correspondence: uwe.scheithauer@ikts.fraunhofer.de; Tel.: +49-351-2553-7671

Abstract: In our study we investigated the additive manufacturing (AM) of ceramic-based Functionally Graded Materials (FGM) by the direct AM technology Thermoplastic 3D-Printing (T3DP). Zirconia components with a varying microstructure were additively manufactured by using thermoplastic suspensions with different contents of pore forming agents (PFA) and were co-sintered defect-free.

Different materials were investigated concerning their suitability as PFA for the T3DP process. Different zirconia-based suspensions were prepared and used for AM of single- and multi-material test components. All samples were sintered defect-free and in the end we could realize a brick wall-like component consisting of dense (<1% porosity) and porous (approx. 5% porosity) zirconia areas to combine different properties in one component.

The T3DP opens the door to AM of further ceramic-based 4D-components like multi-color or multi-material, especially multi-functional components.

Keywords: additive manufacturing (AM); Functionally Graded Materials (FGM); Thermoplastic 3D-Printing (T3DP; ceramics; ceramic-based 4D-components; zirconia; graded microstructure

1. Introduction

The term "4D Printing" was initially used by Tibbits and Sheil [1] and describes a technology, which was developed as a collaboration between the Self-Assembly Lab, Stratasys and Autodesk to manufacture customizable smart materials. By using an additive manufacturing (AM) device, polymer multi-material components with the added capability of shape-transformation from one state to another can be realized. This offers the possibility to include functionalities like actuation, sensing and material logic directly into the components [2]. Additively manufactured multi-material components can transform from any 1D strand or 2D surface into 3D shape or morph from one 3D shape into another. Using only water, heat, light or other simple energy input, this technique offers adaptability and dynamic response for structures and systems of all sizes [2].

In particular, for ceramic components it is very challenging to realize such properties. The reason for this challenge is, the thermal treatment after the AM process being necessary to generate the ceramic properties. In order to obtain a multi-material composite it is fundamental to successfully co-sinter the paired powders in the composite material. Since the sintering of the components is performed at the same temperature and atmosphere, it is a prerequisite for all materials to have a comparable sintering temperature and behavior (starting temperature of sintering, shrinkage

© 2017 by the author(s). Distributed under a Creative Commons CC BY license.

Preprints (www.preprints.org) | NOT PEER-REVIEWED | Posted: 10 October 2017 doi:10.20944/preprints201710.0057.v1

Peer-reviewed version available at Materials 2017, 10, 1368; doi:10.3390/ma10121368

behavior). To avoid critical mechanical stress during cooling, it is also important that the coefficient of thermal expansion of all materials is approximately equal.

Nevertheless it is possible to realize ceramic components with variety of properties by realizing a graded microstructure or material gradients. These composites are called functionally graded material (FGM) [3]. To achieve unprecedented properties of ceramic components we combine the benefits of AM with the benefits of FGM to "4D materials".

In a FGM the properties change gradually with position [3], which generates new fields of application. Graded microstructures as a combination of two or more materials, for example in ceramic-metal composites, result in innovative, multi-functional property combinations, such as hard and ductile, electrically or thermally conductive and insulating, magnetic and nonmagnetic. Conceivable applications are in a variety of industrial and medical fields, for example as cutting tools, wear resistant components, energy and fuel cell components or as bipolar surgical tools [4-9]. Figure 1 shows metal-ceramic components for different applications manufactured by two-components-ceramic injection molding (2C-CIM). Furthermore the manufacturing of two-color components is possible with 2C-CIM (Figure 2).

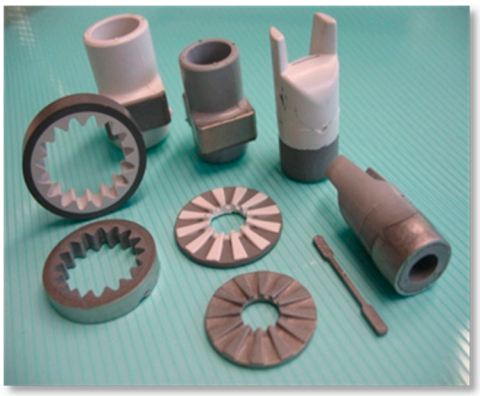

Figure 1. metal-ceramic composites manufactured by 2C-CIM

Figure 2. two-colored zirconia components manufactured by 2C-CIM

Components with different porosities combine different properties in the gradient structure regarding thermal conductivity and capacity, density, mechanical strength, and elastic modulus which shall result e.g. in improved thermal shock properties [10]. Figure 3 shows the SEM-image of a cross-section of a sintered MgO-ZrO2-component with graded porosity and Figure 4 shows the crack surface after a crack deflection during a bending test occurred, due to the graded microstructure and varied Young's modulus [11].

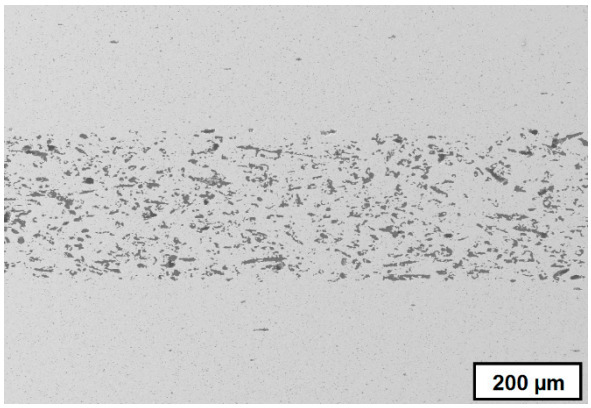

Preprints (www.preprints.org) | NOT PEER-REVIEWED | Posted: 10 October 2017 doi:10.20944/preprints201710.0057.v1

Peer-reviewed version available at Materials 2017, 10, 1368; doi:10.3390/ma10121368

Figure 3. cross-section of sintered MgO-ZrO_2 component with graded microstructure

Figure 4. crack surface of CaAl-Al2O3 component after bending test

AM technologies offer the possibility of a tool-free production of components with extremely complex geometry which cannot be attained by any other shaping technique (Figure 5 and Figure 6). According to ASTM additive manufacturing is a "process of joining material to make objects from 3D model data, usually layer upon layer" [12]. In the plastics industry AM methods are already commercialized to a large extend and the equipment for 3D printing can be even bought for home applications. In the field of metals, more and more materials can be processed as well. For processing ceramic materials, the technical application of AM technologies has been limited so far. However, ceramics have been studied in AM processes ab initio with the development of the different AM technologies since about 25 years [13, 14]. All established AM technologies have also been tested for ceramic materials [15-41]. AM technologies can be classified according to the state of the material that is used – powder materials, liquid materials and solid materials [42, 43] or according to the kind of material deposition and solidification [44]. Lithography-based Ceramic Manufacturing (LCM) allows the AM of dense alumina and zirconia components with extraordinary complex geometries [20-22, 45, 46].

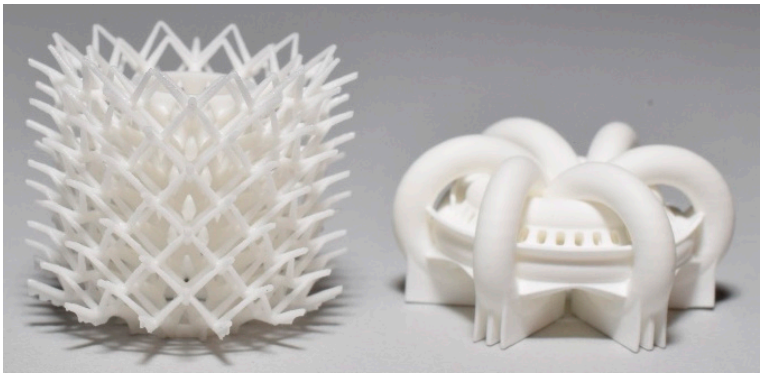

Figure 5. alumina heat exchangers, additively manufactured by Lithography-based Ceramic Manufacturing (LCM)

Figure 6. alumina static mixer, additively manufactured by LCM

Several technologies are known for the production of FGM. Very good overviews are given by Kieback et al. [3], Naebe et al. [47] as well as Moritz et al. [48]. Conventional shaping technologies can be used to produce FGM like powder pressing [49], slip casting [50, 51], powder injection molding [52, 53], tape casting [11, 54-56] or a combination of conventional shaping technologies like inmold-labeling as a combination of tape casting and injection molding [57, 58].

First studies on AM of FGM-components were published about 20 years ago [59-61]. The Multiphase Jet Solidification (MJS)-technology based on thermoplastic binder systems filled with high contents of ceramic particles is nearly similar to the Fused Filament Fabrication (FFF) / Fused Deposition Modeling (FDM®) technology. A hot powder-binder mixture (feedstock) with suitable flow properties was deposited with an extrusion jet moved in two dimensions. During cooling the mixture solidified and a free-standing body was formed. By using a two piston construction

Preprints (www.preprints.org) | NOT PEER-REVIEWED | Posted: 10 October 2017 doi:10.20944/preprints201710.0057.v1

Peer-reviewed version available at Materials 2017, 10, 1368; doi:10.3390/ma10121368

combined with a small static mixing chamber, the powder composition was varied from layer to layer and three dimensional graded SiC-TiC components could be formed [59, 60].

Zhang et al. used Laminated Object Manufacturing (LOM) to manufacture TiC-Ni-FGMs. Green tapes with different compositions were produced, cut by a laser, stacked and laminated [61].

Another approach is the functionalization of additively manufactured and sintered ceramic components subsequent to its generation. Figure 7 shows an alumina component manufactured by Lithography-based Ceramic Manufacturing (LCM), sintered at 1600 °C and subsequently functionalized with electrically conductive heater structures by Aerosol-printing [48].

Figure 7. post-functionalized additively manufactured alumina component

Direct AM technologies are more suitable for AM of multi-material components than indirect AM technologies because of the selective deposition of the used material. The latter ones are based on the selective solidification of material which was deposited all-over the entire layer. Therefore the areas which have not been solidified are occupied by non-solidified material which have to be removed before a second material can be deposited in these areas. Using direct AM technologies a second material and further ones can be deposited directly beside the already deposited and solidified first material.

In our study we investigated the AM of ceramic-based FGM by the direct AM technology Thermoplastic 3D-Printing (T3DP). Zirconia components with a varying microstructure were additively manufactured by using thermoplastic suspensions with different contents of pore forming agents (PFA) and were co-sintered defect-free.

2. Experimental

2.1. Thermoplastic 3D-Printing

T3DP bases on the selective deposition of particle-filled thermoplastic suspensions not over the entire surface, but instead only at the required spots [62]. Different suspensions can be deposited beside each other in each single layer and bulk material as well as property gradients can be realized within the additively manufactured green components [63-65].

Several heatable dispensing units which are moved over a fixed platform in all three spatial directions deposit the suspensions. The thermoplastic suspensions are heated until they are in a flowable state. They are deposited at the desired position, and solidify immediately on cooling as well as lacking shear forces. The solidification takes place almost independently of the physical properties of the used powders so even hard metal components can be manufactured [66]. Several

Preprints (www.preprints.org) | NOT PEER-REVIEWED | Posted: 10 October 2017 doi:10.20944/preprints201710.0057.v1

Peer-reviewed version available at Materials 2017, 10, 1368; doi:10.3390/ma10121368

supply containers and dispensing units can be used for the localized deposition of different materials, including supporting structures, in one and the same component.

2.2. Used materials

As ceramic material the yttria-stabilized zirconia powders TZ-3Y-E by Tosoh Corporation of Japan was used.

Three different materials were investigated concerning their behavior as a PFA. ARBOCEL UFC100 of the company J. Rettenmaier Söhne GmbH + Co KG is a cellulose powder based on cellulose fibers with an average particle size of 6 µm – 12 µm. The decomposition temperature of this material is about 200 °C and corresponds to the decomposition temperature of a second polysaccharide (PS) powder (starch) with rounder shape and a maximum diameter below 25 µm. CERETAN MA 7008 (Münzing Chemie GmbH) is an amide of a carboxylic acid with a decomposition temperature of about 150 °C and a d_{99} of 8 µm. It was selected to investigate the suitability as PFA in spite of the significant lower decomposition temperature.

2.3. Feedstock preparation

The different zirconia suspensions were prepared by dispersing the powder together with the PFA in a thermoplastic binder system basing on a mixture of molten paraffin and beeswax. The dispersion and homogenization took place in a heatable dissolver (Dissolver DISPERMAT CA 20-C, VMA-Getzmann GmbH) by stirring for 4 h. Suspensions with 36 vol.-% and 40 vol.-% were prepared.

The content of PFA was varied for each material. Table 1 summarizes the composition of the different thermoplastic suspensions.

Table 1. composition of used thermoplastic suspensions

zirconia content / vol.-%	36	40	36	36	38	38
used PFA	---	---	poly-saccharide	poly-saccharide	CERETAN MA 7008	UFC100
d_{50} of PFA / µm	---	---	7	7	< 8	8
content of PFA / vol.-%	---	---	5	10	2	2
binder content / vol.-%	64	60	59	54	60	60

2.4. Preparation of single- and multi-material test components

The test samples were additively manufactured by using micro dispensing systems of Vermes, Germany. Four of them are mounted on our xyz-laboratory rig, which can operate alternately. One dispensing system was used to manufacture the single-material components, two of them were used for the manufacturing of multi-material test components.

The dispensing parameters had to be adjusted for each suspension due to the different rheological behavior. The deposition of the droplets happened with a frequency up to 100 Hz and the axes were moved with a maximal velocity of 50 mm/s.

The green samples were debinded in a powder bed at a very low heating rate, in a first step under air-atmosphere up to 270°C (heating rate 4 K/h) and then after removing the powder in a second step under air-atmosphere up to 900°C (12 K/h). Afterwards the components were sintered under air-atmosphere at 1350 °C (3 K/min) for 2 hours.

2.5. Characterization methods

The particle size distribution of the utilized powders and PFA were measured by a laser diffraction method (Mastersizer 2000, Malvern Instruments Ltd., United Kingdom). Electron scanning microscopy images have been used to characterize the shape of the particles.

To characterize the rheological behavior of the zirconia suspensions, a rheometer (Modular Compact Rheometer MCR 302; Anton Paar, Graz, Austria) adjustable between -25 to 200°C with a

Preprints (www.preprints.org) | NOT PEER-REVIEWED | Posted: 10 October 2017 doi:10.20944/preprints201710.0057.v1

Peer-reviewed version available at Materials 2017, 10, 1368; doi:10.3390/ma10121368

plate/plate measuring system was used. The flow behavior was analyzed with an increasing shear rate (0–10000 s-1) and at varying temperatures between 85°C and 100°C. The torque was measured and the viscosity calculated.

FESEM images of the sintered samples have been utilized to evaluate the samples density and porosity. The FESEM images were converted into binary images by means of an open source software called Image J, i.e. all pores were converted into black pixels and the ceramic particles into white pixels. In order to calculate the samples porosity the software compares the number of the black and white pixels of a converted image of a samples cross sections.

Additionally, the density was measured by Archimedes' principle.

3. Results and discussions

3.1. FESEM-studies of used materials

The measured average particle size (d_{50}) of the zirconia powder was with 0.37 µm by about one order of magnitude larger than the average particle size stated by Tosoh (d_{50} = 0.04 µm). FESEM-images showed that the untreated powder consists of very big granulates (diameter up to 100 µm) which were crushed during the ultrasonic-treatment before the laser diffraction (Figure 8). Still, the applied treatment was just insufficient regarding the deagglomeration of all the particles. But during the feedstock preparation very high shear forces were realized which should deagglomerate all particles.

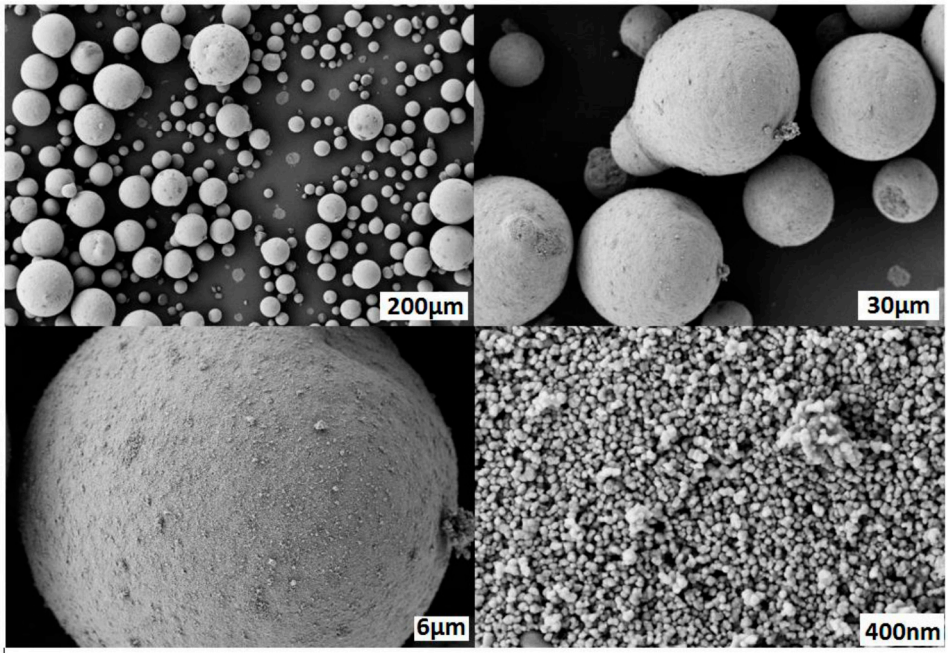

Figure 8. FESEM-images of untreated zirconia powder

Figure 9 and Figure 10 show FESEM-images of two materials used as a PFA. ARBOCEL UFC100 bases on cellulose fibers and the particles have a fiber-fragments-like shape (Figure 9). The particles of the PS powder have a polyhedral-like shape (Figure 10). The particle size investigated on FESEM-images varied between 5 µm and 20 µm.

Preprints (www.preprints.org) | NOT PEER-REVIEWED | Posted: 10 October 2017 doi:10.20944/preprints201710.0057.v1

Peer-reviewed version available at Materials 2017, 10, 1368; doi:10.3390/ma10121368

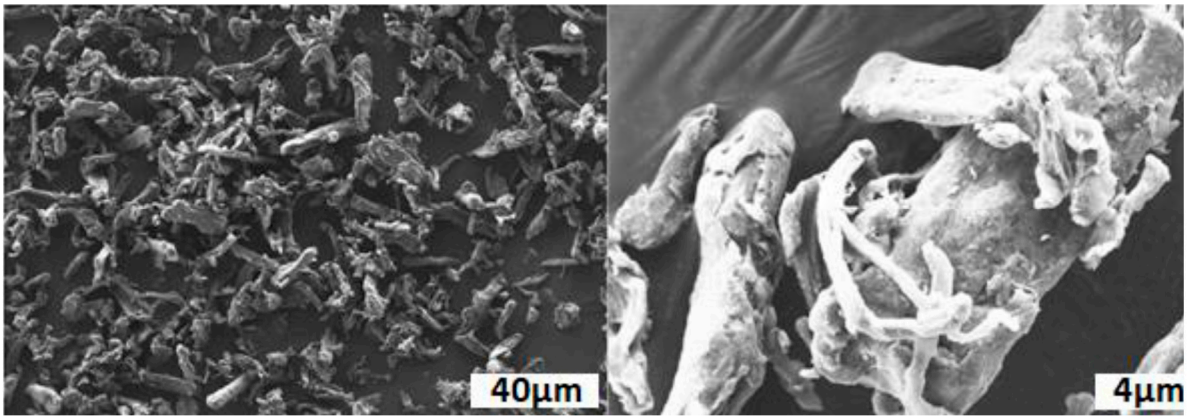

Figure 9. FESEM-images of ARBOCEL UFC100

189

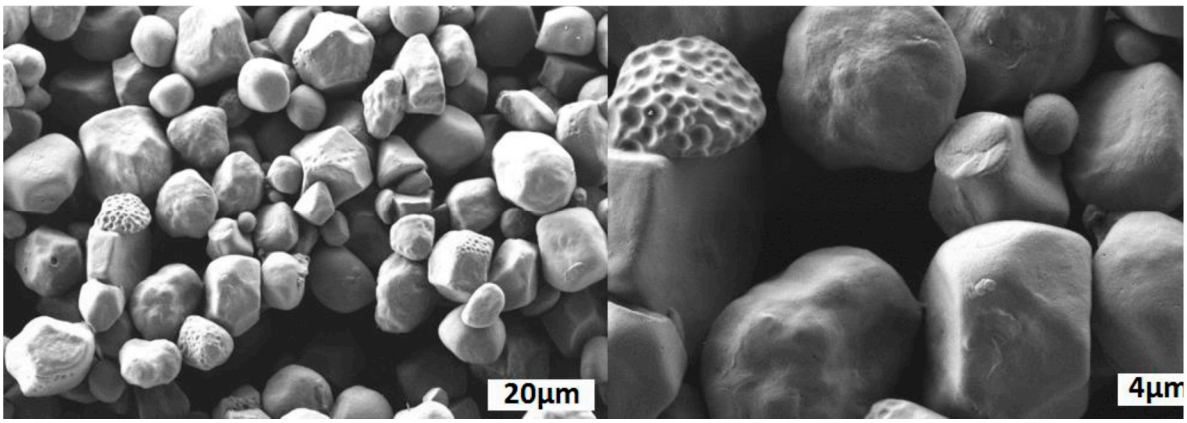

Figure 10. FESEM-images of polysaccharide powder

190

191 The FESEM-images of the used PFA materials gives an explanation for the content of PFA which
192 could be realized in the different suspensions. With the starch powder (polysaccharide) a significant
193 higher content of PFA (up to 10 vol.-%) could be realized. For the other two materials the viscosity
194 increased significant for contents of more than 2 vol.-%. Probably this results from the higher and
195 rough surface of CERETAN MA 7008 and UFC 100 compared to the smooth surface of the starch
196 powder.

197 *3.2. Rheological behavior of the thermoplastic suspensions*

198 The results of the rheological measurements of the two zirconia suspensions without any content
199 of a PFA are summarized in Figure 11. The dynamic viscosity is displayed as function of the shear
200 rate in a double logarithmic plot with a shear rate range between 0.1 and 10000 s-1. All suspensions
201 show a shear thinning behavior at both temperatures. With increasing solid content and decreasing
202 temperature the dynamic viscosity increases.
203

Preprints (www.preprints.org) | NOT PEER-REVIEWED | Posted: 10 October 2017 doi:10.20944/preprints201710.0057.v1

Peer-reviewed version available at Materials 2017, 10, 1368; doi:10.3390/ma10121368

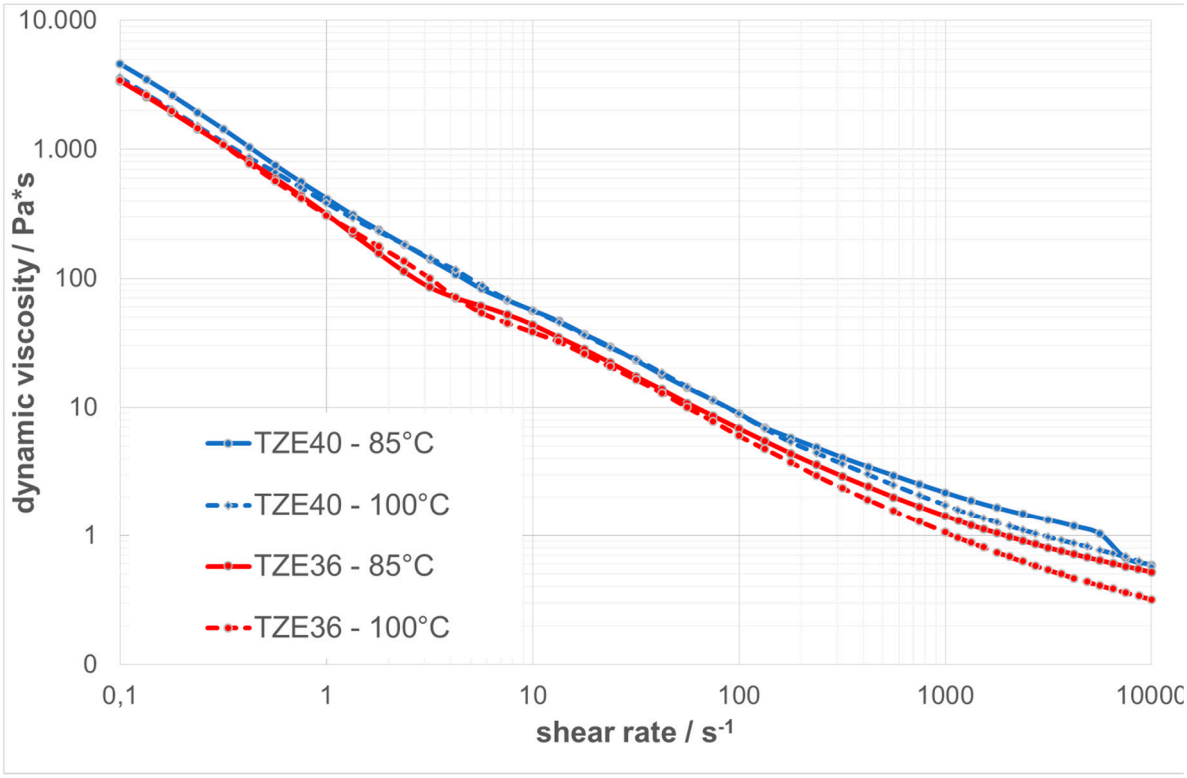

Figure 11. rheological behavior of zirconia suspensions without any PFA

204

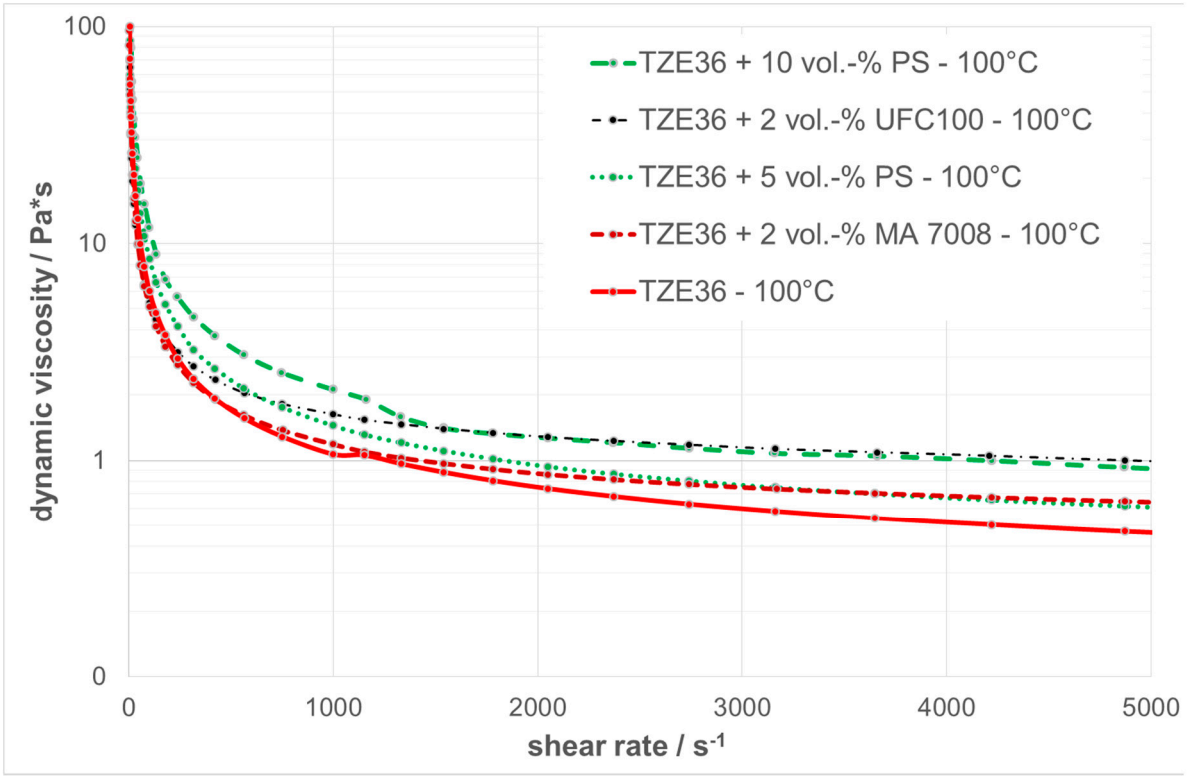

Figure 12. rheological behavior of zirconia suspensions with and without PFA at 100 °C

205

206 Figure 12 shows the dynamic viscosities as function of the shear rate at a temperature of 100 °C
207 for the different suspensions with and without PFA. The suspension without any PFA has the lowest

Preprints (www.preprints.org) | NOT PEER-REVIEWED | Posted: 10 October 2017 doi:10.20944/preprints201710.0057.v1

Peer-reviewed version available at Materials 2017, 10, 1368; doi:10.3390/ma10121368

viscosity and by adding PFA the viscosity increases. However, all suspensions show a shear thinning behavior with a dynamic viscosity of 1 Pa*s or lower at a shear rate of 5000 s-1 and therefore can be utilized for T3DP. Table 2 summarizes the measured viscosities of the suspensions at different shear rates and temperatures.

Table 2. dynamic viscosity of the suspensions at different shear rates

zirconia content / vol.-%	PFA: kind and content / vol.-%	tempe-rature / °C	shear rate / s^{-1}					
			0,1	1	10	10^2	10^3	10^4
36	---	85	3400	312	43,80	6,86	1,43	0,52
		100	3420	309	38,30	6,03	1,07	0,32
40	---	85	4600	414	56,60	8,98	2,16	0,59
		100	3630	386	56,00	8,96	1,75	0,57
36	polysaccharide 5	85	3770	355	56,60	8,26	1,80	0,59
		100	2510	240	42,40	8,48	1,45	0,45
36	polysaccharide 10	85	1800	374	79,30	10,30	2,47	0,65
		100	5420	513	79,60	11,80	2,12	0,53
38	MA7008 2	85	2220	265	38,50	6,56	1,83	0,62
		100	1130	140	32,50	5,11	1,18	0,43
38	UFC100 2	85	1770	214	31,60	5,34	1,63	0,60
		100	1210	143	31,40	4,83	1,15	0,48

3.3. single-material components

After a screening of the deposition parameters it was realizable to manufacture test components for each suspension. Figure 13 shows three views of a complex structure additively manufactured by T3DP with the zirconia suspension without a PFA. The shown test components were realized without a prerequisite utilization of any support structure respectively support material. After sintering, the wall thickness of this structure was less than 0.8 mm. The manufacturing time for the green component was approximately 30 minutes.

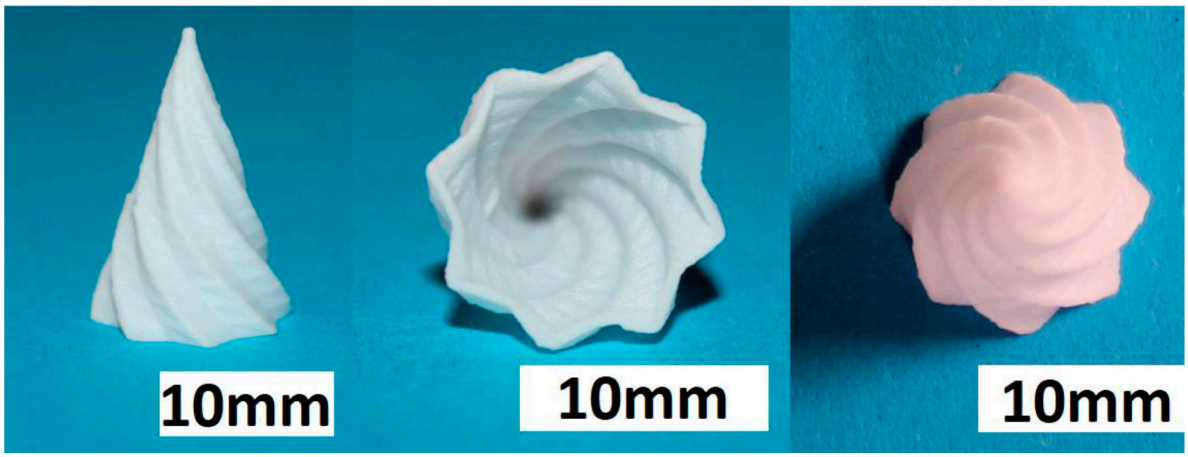

Figure 13. sintered zirconia test component additively manufactured by T3DP with 36 vol.-% zirconia particles in the suspension and without PFA; three different views

The FESEM-images of the cross-section of sintered zirconia test components additively manufactured by T3DP with 36 vol.-% zirconia particles and without any PFA in the suspension are

Preprints (www.preprints.org) | NOT PEER-REVIEWED | Posted: 10 October 2017 doi:10.20944/preprints201710.0057.v1

Peer-reviewed version available at *Materials* **2017**, *10*, 1368; doi:10.3390/ma10121368

shown in Figure 14. A very homogeneous microstructure almost without any porosity can be seen. By utilizing ImageJ and five different FESEM-images an average porosity of 0.11 +/- 0.04% was calculated. With Archimedes' principle an average outer density of 5.90 +/- 0.04 g/cm³ and an average inner density of 5.93 +/- 0.05 g/cm³ was investigated for 14 test samples.

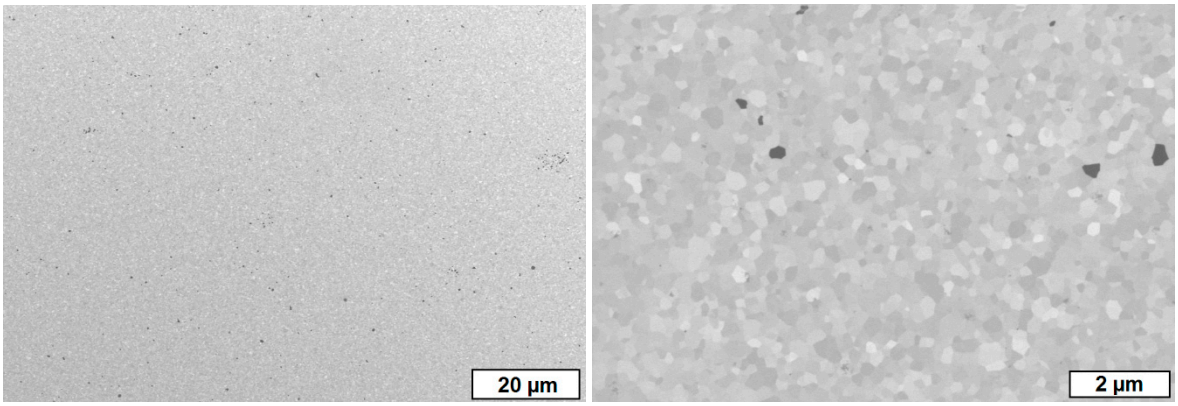

Figure 14. FESEM-images of sintered zirconia test components additively manufactured by T3DP with 36 vol.-% zirconia particles and without PFA in the suspension

In addition test samples of the suspensions with PFA were manufactured. Figure 15 shows two views of a green sample including 5 vol.-% PS as PFA, for instance.

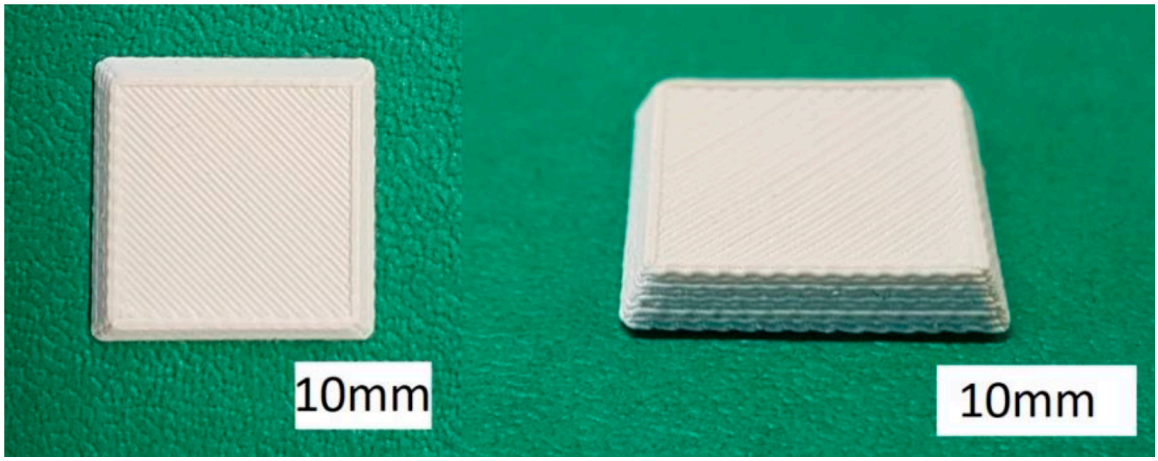

Figure 15. green zirconia test components with 5 vol.-% PS as a PFA

The FESEM-images of the sintered test components additively manufactured by T3DP with the suspensions which included 5 vol.-% PS (left) and 10 vol.-% PS (right) as PFA are summarized in Figure 16. The images show a homogeneous distribution of the single pores with a nearly round shape resulting from the polyhedron-like shape of the PS-powder as PFA. The average porosities calculated with ImageJ on five images each are 5.02 +/- 0.43 % and 10.72 +/- 0.87 %, respectively. These correspond almost exactly to the content of added PFA in the suspensions (5 vol.-% and 10 vol.-%).

Preprints (www.preprints.org) | NOT PEER-REVIEWED | Posted: 10 October 2017 doi:10.20944/preprints201710.0057.v1

Peer-reviewed version available at Materials 2017, 10, 1368; doi:10.3390/ma10121368

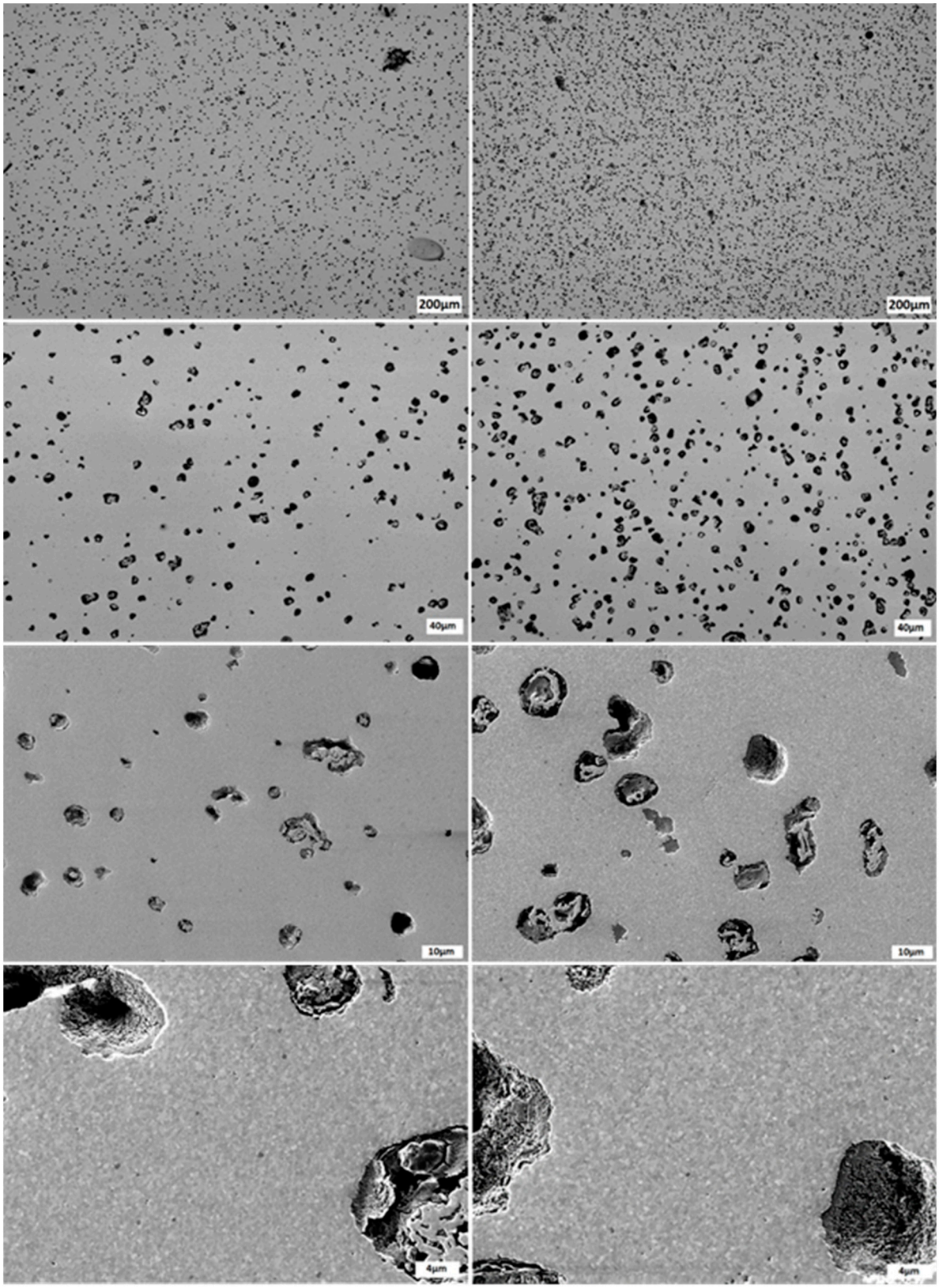

Figure 16. FESEM-images of cross-sections of sintered zirconia test samples with 5 vol.-% PS and 10 vol.-% PS as PFA in the suspension

242
243 However, not every of the used materials operated as a PFA. Figure 17 shows FESEM-images of
244 sintered zirconia components additively manufactured by T3DP and a suspension with 2 vol.-% of

Preprints (www.preprints.org) | NOT PEER-REVIEWED | Posted: 10 October 2017 doi:10.20944/preprints201710.0057.v1

Peer-reviewed version available at Materials 2017, 10, 1368; doi:10.3390/ma10121368

CERETAN MA 7008 as PFA. After sintering only a few pores can be detected which are located in the image in an almost horizontal row. Probably these are resulting from trapped air bubbles between two layers during the manufacturing process.

The decomposition temperature of CERETAN MA 7008 (about 150 °C) seems to be too low to be utilized as a PFA for T3DP. The material is removed during the first debinding step and probably due to a still lasting thermoplastic behavior of the suspension at this temperature, rearrangement processes can occur driven by capillary forces. Subsequently, the remaining pores are eliminated during the final sintering step. This topic has to be investigated in further studies.

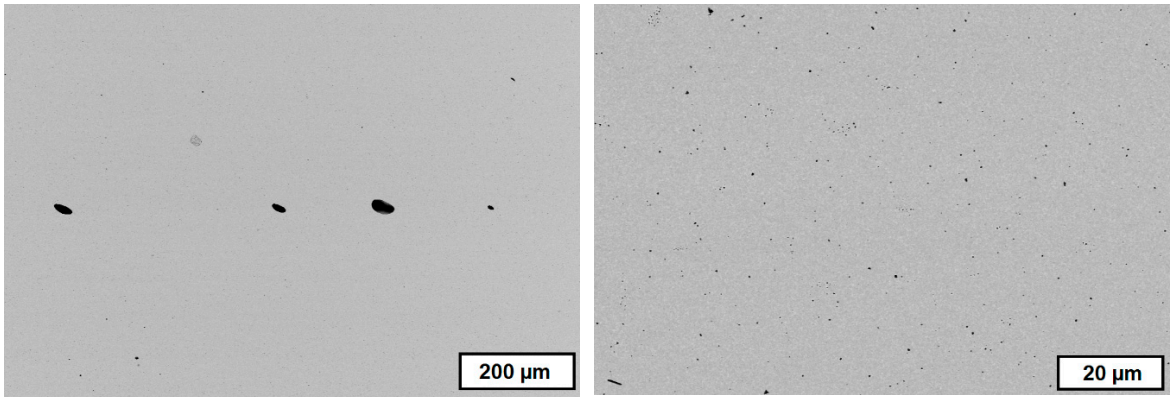

Figure 17. FESEM-images of cross-section of test component with CERETAN MA 7008 as PFA

3.4. ceramic-based 4D-components

To demonstrate the additive manufacturing of zirconia-based 4D-components we manufactured components with a brick wall design. Figure 18 is showing a CAD-drawing of the design. The brighter areas were manufactured with 5 vol.-% PS as PFA and the dark areas were manufactured with the pure zirconia suspension (36 vol.-% solid load, no PFA). The resulting defect-free sintered components are shown in Figure 19.

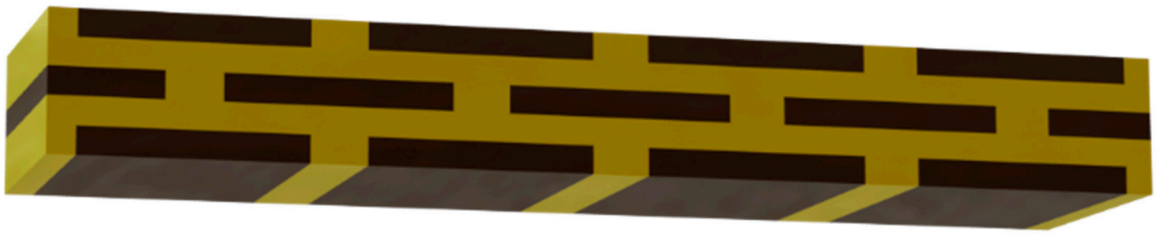

Figure 18. CAD-drawing of 4D-component: brick wall-like test component

Preprints (www.preprints.org) | NOT PEER-REVIEWED | Posted: 10 October 2017 doi:10.20944/preprints201710.0057.v1

Peer-reviewed version available at Materials 2017, 10, 1368; doi:10.3390/ma10121368

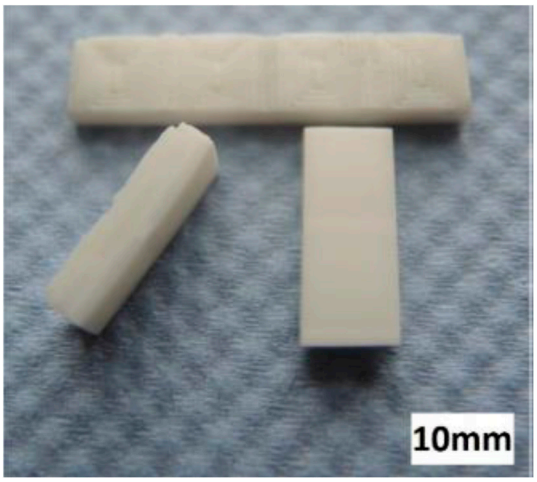

Figure 19. sintered zirconia 4D-components

FESEM-images of cross-sections of these 4D-components show clearly distinguishable areas at the interface between the two former suspensions (Figure 20). Thus, regardless of the drop-bound deposition of the material the arrangement of the different microstructure can be realized very precisely.

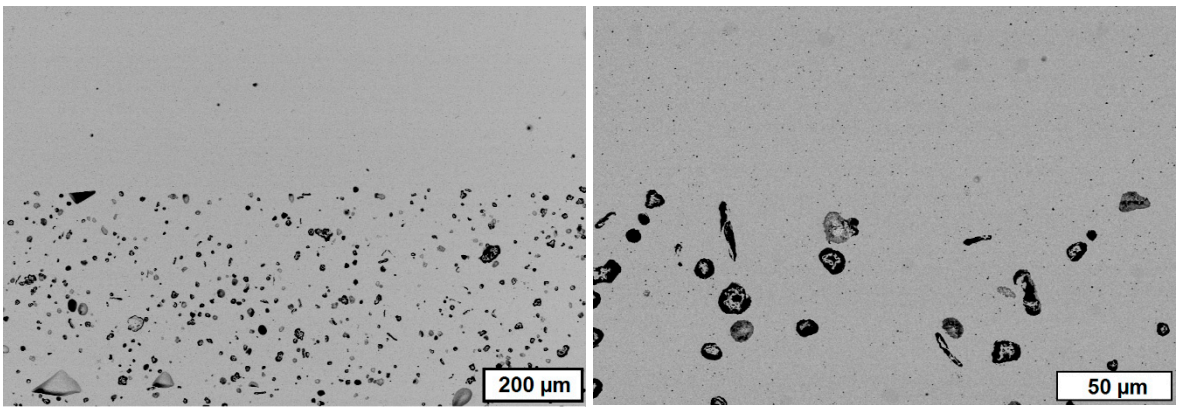

Figure 20. FESEM-images of cross-section of sintered zirconia 4D-component; interface between dense and porous area; left: overview; right: detail

To illustrate the difference in porosity we placed the zirconia-based 4D-components in front of a light spot (Figure 21). While the porous areas shine darker because of the light deflection and reflection, the denser areas show the opposite behavior by appearing nearly translucent.

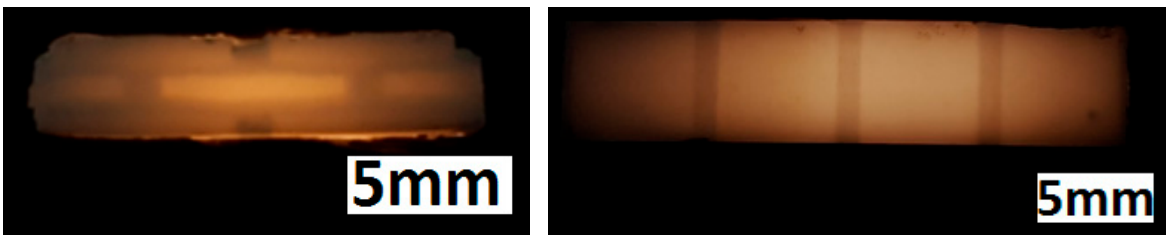

Figure 21. sintered zirconia 4D-component in front of a light spot with two different microstructures (darker areas: porous; brighter areas: dense); left: side view (section); right: top view

Preprints (www.preprints.org) | NOT PEER-REVIEWED | Posted: 10 October 2017 doi:10.20944/preprints201710.0057.v1

Peer-reviewed version available at Materials 2017, 10, 1368; doi:10.3390/ma10121368

4. Conclusions

In our study we could show that it is possible to combine AM and FGM to zirconia-based 4D-components. We used the T3DP technology as directly working AM technology to selectively deposit two different materials besides each other. This offers the possibility to combine suspensions with different contents of a PFA to realize components with dense and porous areas inside.

Different materials were investigated concerning their suitability as a PFA for the T3DP process. Different zirconia-based suspensions were prepared and used for AM of single- and multi-material test components. All samples were sintered defect-free and in the end we could realize a brick wall-like component consisting of dense (< 1 % porosity) and porous (approx. 5 % porosity) zirconia areas to combine different properties in one component.

The T3DP opens the door to AM of further ceramic-based 4D-components like multi-color or multi-material components which will be presented in further papers.

Acknowledgments: This project has received funding from the European Union's Horizon 2020 Research and Innovation Programme under Grant Agreement No 678503.

References

1. Tibbits, S.; Sheil, B. 4D Printing: Multi-Material Shape Change, *Architectural Design*. January **2014**, *Vol.84 (1)*, pp.116-121, DOI: 10.1002/ad.1710
2. http://www.selfassemblylab.net/4DPrinting.php, website, 17/10/05
3. Kieback, B.; Neubrand, A.; Riedel, H. Processing techniques for functionally graded materials. *Materials Science and Engineering: A*, **2003**, *362, Issues 1–2*, 81–106, DOI: 10.1016/S0921-5093(03)00578-1
4. Lee, H.C.; Potapova, Y.; Lee, D. A core-shell structured, metal-ceramic composite supported Ru catalyst for methane steam reforming. *J of Power Sources*, **2012**, *216*, 256-260, DOI: 10.1016/j.jpowsour.2012.05.056
5. Molin, S.; Tolczyk, M.; Gazda, M.; Jasinski, P. Stainless steel/yttria stabilized zirconia composite supported solid oxide fuel cell. *J. Fuel Cell Sci. Technol.*, **2011**, *8*, 1-5, DOI: 10.1016/j.jpowsour.2016.05.076
6. Roberts H.W.; Berzins D.W.; Moore B.K.,; Charlton D.G. Metal-Ceramic Alloys in Dentistry: A Review. *Journal of Prosthodontics*, **2009**, *18, Issue 2*, 188–194, DOI: 10.1111/j.1532-849X.2008.00377.x
7. Largiller, G.; Bouvard, D.; Carry, C.P.; Gabriel, A.; Müller, J.; Staab, C. Deformation and cracking during sintering of bimaterial components processed from ceramic and metal powder mixes. Part I: Experimental investigation, *Mechanics of Materials*, **2012**, *53*, 123-131, DOI: 10.1016/j.mechmat.2012.04.002
8. Meulenberg, W. A.; Mertens, J.; Bram, M.; Buchkremer, H.-P.; Stöver, D. Graded porous TiO_2 membranes for micro-filtration. *Journal European Ceramic Society*, **2006**, *26*, 449-454, DOI: 10.1016/j.jeurceramsoc.2005.06.035
9. Baumann, A.; Moritz, T.; Lenk, R. Multi component powder injection moulding of metal-ceramic-composites. Proceedings of the Euro International Powder Metallurgy Congress and Exhibition 2009, Copenhagen, Denmark
10. Hein, J.; Scheithauer, U.; Haderk, K.; Kuna, M.; Michaelis, A. Prospect of a new generation of refractories made by ceramic multilayer technology. *Refractories Manual*, **2012**, *2*, 91-95
11. Scheithauer, U.; Schwarzer, E.; Slawik, T.; Richter, H.-J.; Moritz, T.; Michaelis, A. Functionally Graded Materials Made by Water-Based Multilayer Technology. *Refractories Worldforum*, **2016**, *Volume 8, Issue 2*, 95 – 101
12. ASTM-Standard F2792 -12a: Standard Terminology for Additive Manufacturing Technologies. *ASTM International Distributed under ASTM license by Beuth publisher*, **March 1**, **2012**
13. Lakshminarayan, U.; Ogrydiziak, S.; Marcus, H.L. Selective lasersintering of ceramic materials. Proceedings of Solid Free-Form Symposium 1990, Austin, Texas, USA, 16-26
14. Lauder, A.; Cima, M.J.; Sachs, E. Fan, T. Three dimensional printing: surface finish and microstructure of rapid prototyped components. Materials Research Society Symposium Proceedings 1992, *249*, 331-336
15. Pham-Gia, K.; Rossner, W.; Wessler, B.; Schäfer, M.; Schwarz, M. Rapid Prototyping of high-density alumina ceramics using stereolithography. *cfi/ Ber. DKG*, **2006**, *83*, 36-40

Preprints (www.preprints.org) | NOT PEER-REVIEWED | Posted: 10 October 2017 doi:10.20944/preprints201710.0057.v1

Peer-reviewed version available at Materials 2017, 10, 1368; doi:10.3390/ma10121368

16. Chartier, T.; Duterte, C.; Delhote, N.; Baillargeat, D.; Verdeyme, S.; Delage, C.; Chaput, C.J. Fabrication of millimeter wave components via ceramic stereo- and microstereolithography processes. *J. Am. Ceram. Soc.*, **2008**, *91*, 2469–2474, DOI: 10.1111/j.1551-2916.2008.02482.x
17. Griffith, M.L.; Halloran, J.W. Freeform fabrication of ceramics via stereolithography. *J. Am. Ceram. Soc.*, **1996**, *79*, 2601-2608, DOI: 10.1111/j.1151-2916.1996.tb09022.x
18. Licciulli, A.; Corcione, C.E.; Greco, A.; Amicarelli, V.; Maffezzoli, A. Laser stereolithography of ZrO_2 toughened Al_2O_3. *J. Europ. Ceram. Soc.*, **2005**, *25*, 1581-1589, DOI: 10.1016/j.jeurceramsoc.2003.12.024
19. de Hazan, Y.; Thänert, M.; Trunec, M.; Misak, J. Robotic deposition of 3d nanocomposite and ceramic fiber architectures via UV curable colloidal inks. *J. Europ. Ceram. Soc.*, **2012**, *32*, 1187-1198, DOI: 10.1016/j.jeurceramsoc.2011.12.007
20. Felzmann, R.; Gruber, S.; Mitteramskogler, G.; Tesavibul, P.; Boccaccini, A.R.; Liska, R.; Stampfl, J. Lithography-based additive manufacturing of cellular ceramic structures. *Adv. Eng. Mater.*, **2012**, *14*, 1052-1058, DOI: 10.1002/adem.201200010
21. Fischer, U. K.; Moszner, N.; Rheinberger, V.; Wachter, W.; Homa, J.; Längle, W. Lichthärtende Keramikschlicker für die stereolithographische Herstellung von hochfesten Keramiken (light curing ceramic suspensions for stereolithography of high-strength ceramics), european patent EP 2404590A1, published 11.01.2012
22. Homa, J. Rapid Prototyping of high-performance ceramics opens new opportunities for the CIM industry. *Powder Injection Moulding International*, **2012**, *6 (3)*, 65-68
23. Lenk, R.; Nagy, A.; Richter, H.-J.; Techel, A. Material development for laser sintering of silicon carbide. *cfi/ Ber. DKG*, **2006**, *83*, 41-43
24. Regenfuss, P.; Ebert, R.; Exner, H. Laser Micro Sintering - a versatile instrument for the generation of microparts. *Laser Technik Journal*, **2007**, *4*, 26-31, DOI: 10.1002/latj.200790139
25. Hagedorn, Y.-C.; Wilkes, J.; Meiners, W.; Wissenbach, K.; Poprawe, R. Net shaped high performance oxide ceramic parts by selective laser melting. *Phys. Procedia*, **2010**, *5*, 587–594, DOI: 10.1016/j.phpro.2010.08.086
26. Wu, Y.; Du, J.; Choy, K.-L.; Hench, L.L. Laser densification of alumina powder beds generated using aerosol spray deposition. *J. Europ. Ceram. Soc.*, **2007**, *27*, 4727-4735, DOI: 10.1016/j.jeurceramsoc.2007.02.219
27. Goodridge, R.D.; Lorrison, J.C.; Dalgarno, K.W.; Wood, D.J. Comparison of direct and indirect selective laser sintering of porous apatite mullite glass ceramics. *Glass Technology*, **2004**, *45*, 94-96
28. Gbureck, U.; Hoelzel, T.; Biermann, I.; Barralet, J.; Grover, L.M. Preparation of tricalcium phosphate/calcium pyrophosphate structures via rapid prototyping. *J. Mater. Sci.: Mater. Med.*, **2008**, *19*, 1559-1563, DOI: 10.1007/s10856-008-3373-x.
29. Seitz, H.; Rieder, W.; Irsen, S.; Leukers, B.; Tille, C. Three-dimensional printing of porous ceramic scaffolds for bone tissue engineering. *Biomed. Mater. Res., Part B: Appl. Biomater.*, **2005**, *74B*, 782-788, DOI: 10.1002/jbm.b.30291
30. Khalyfa, A.; Meyer, W.; Schnabelrauch, M.; Vogt, S.; Richter, H.-J. Manufacturing of biocompatible ceramic bone substitutes by 3D-printing. *cfi/ Ber. DKG*, **2006**, *83*, 23-26
31. Deisinger, U.; Irlinger, F.; Pelzer, R.; Ziegler, G. 3D-printing of HA-scaffolds for the application as bone substitute material. *cfi/ Ber. DKG*, **2006**, *83*, 75-78
32. Dombrowski, F.; Caso, P.W.G.; Laschke, M.W.; Klein, M.; Guenster, J.; Berger, G. 3-D printed bioactive bone replacement scaffolds of alkaline substituted ortho-phosphates containing meta- and di-phosphates, *Key Engineering Materials*, **2013**, *529-530*, 138-142, DOI: 10.4028/www.scientific.net/KEM.529-530.138
33. Zocca, A.; Gomes, C.M.; Bernardo, E.; Müller, R.; Günster, J.; Colombo, P. LAS glass–ceramic scaffolds by three-dimensional printing. *J. Europ. Ceram. Soc.*, **2013**, *33*, 1525-1533, DOI: 10.1016/j.jeurceramsoc.2012.12.012
34. Sadeghian, Z.; Heinrich, J.G.; Moztarzadeh, F. Direct Laser Sintering of Hydroxyapatite Implants by Layerwise Slurry Deposition (LSD). *cfi/Ber. DKG*, **2004**, *81 (12)*, E39-E43
35. Cappi, B.; Oezkol, E.; Ebert, J.; Telle, R. Direct inkjet printing of Si_3N_4: Characterization of ink, green bodies, and microstructure. *J. Europ. Ceram. Soc.*, **2008**, *28*, 2625-2628, DOI: 10.1016/j.jeurceramsoc.2008.03.004
36. Ebert, J.; Özkol, E.; Zeichner, A.; Uibel, K.; Weiss, Ö.; Koops, U.; Telle, R.; Fischer, H. Direct Iinkjet printing of dental prostheses made of zirconia. *J. Dent. Res.*, **2009**, *88*, 673-676, DOI: 10.1177/0022034509339988.
37. Allahverdi, M.; Danforth, S.C.; Jafari, M.; Safari, A. Processing of advanced electroceramic components by fused deposition technique. *J. Europ. Ceram. Soc.*, **2001**, *21*, 1485-1490, DOI: 10.1016/S0955-2219(01)00047-4

Preprints (www.preprints.org) | NOT PEER-REVIEWED | Posted: 10 October 2017 doi:10.20944/preprints201710.0057.v1

Peer-reviewed version available at Materials 2017, 10, 1368; doi:10.3390/ma10121368

38. Bose, S.; Darsell, J.; Hosick, H.; Yang, L.; Sarkar, D.K.; Bandyopadhyay, A. Processing and characterization of porous alumina scaffolds. *J. Mater. Sci.: Mater. Med.*, **2002**, *13*, 23-28, DOI: 10.1023/A:1013622216071
39. Schlordt, T.; Schwanke, S.; Keppner, F.; Fey, T.; Travitzky, N.; Greil, P. Robocasting of alumina hollow filament lattice structures. *J. Europ. Ceram. Soc.*, **2013**, *33*, 3243–3248, DOI: 10.1016/j.jeurceramsoc.2013.06.001
40. Cai, K.; Roman-Manso, B.; Smay, J.E.; Zhou, J.; Osendi, M.I.; Belmonte, M.; Miranzo, P. Geometrically complex silicon carbide structures fabricated by robocasting. *J. Am. Ceram. Soc.*, **2012**, *95*, 2660-2666, DOI: 10.1111/j.1551-2916.2012.05276.x
41. Polsakiewicz, D.; Kollenberg, W. Process and materials development for functionalized printing in three dimensions (FP-3D). *refractories WORLDFORUM*, **2012**, *4*, 1-8
42. Chartier T.; Badev, A. Rapid Prototyping of Ceramics. In *Handbook of Advanced Ceramics Elsevier*, 2nd ed., Somiya, S., Elsevier Inc., Oxford, UK, 2013
43. Travitzky, N.; Bonet, A.; Dermeik, B.; Fey, T.; Filbert-Demut, I.; Schlier, L.; Schlordt, T.; Greil, P. Additive Manufacturing of ceramic-based material. *Advanced Engineering Materials*, **2014**, *16*, 729-754, DOI: 10.1002/adem.201400097
44. Zocca, A.; Colombo, P.; Gomes, C. M.; Günster, J. Additive Manufacturing of Ceramics: Issues, Potentialities, and Opportunities. *Journal of the American Ceramic Society*, **2015**, *Vol.98 (7)*, 1983-2001, DOI: 10.1111/jace.13700
45. Scheithauer, U.; Schwarzer, E.; Ganzer, G.; Körnig, A.; Beckert, W.; Reichelt, E.; Jahn, M.; Härtel, A.; Richter, H.-J.; Moritz, T.; Michaelis, A. Micro-reactors made by Lithography-based Ceramic Manufacturing (LCM). Proceedings of 11th International Conference on Ceramic Materials and Components for Energy and Environmental Applications 2015, Vancouver, Ceramic Transactions, 2016, 258, The American Ceramic Society, DOI: 10.1002/9781119236016
46. Scheithauer, U.; Schwarzer, E.; Moritz, T.; Michaelis, A. Additive Manufacturing of ceramic heat exchanger - Opportunities and limits of the Lithography-based Ceramic Manufacturing (LCM). *Journal of materials engineering and performance: design, process, characterization, evaluation*, **2017,** DOI: 10.1007/s11665-017-2843-z
47. Naebe, M.; Shirvanimoghaddam, K. Functionally graded materials: A review of fabrication and properties. *Applied Materials Today*, **2016**, *Volume 5*, 223-245, DOI: 10.1016/j.apmt.2016.10.001
48. Moritz, T.; Scheithauer, U.; Mannschatz, M.; Ahlhelm, A.; Abel, J.; Schwarzer, E.; Pohl, M.; Müller-Köhn, A. Material- and process hybridization for multifunctional ceramic and glass components. *Ceramic Applications*, **2017**, *Vol.5, No.2*, 66-71
49. Mortensen, A.; Suresh, S. Functionally graded metals and metal-ceramic composites: Part 1 Processing. *International Materials Reviews*, **1995**, *40, No.6*, 239-265, DOI: 10.1179/imr.1995.40.6.239
50. Moya, J.S.; Sánchez-Herencia, A.J.; Requena, J.; Moreno, R. Functionally gradient ceramics by sequential slip casting. *Materials Letters*, **1992**, *14 (5)*, 333-335, DOI: 10.1016/0167-577X(92)90048-O
51. Moya, J.S.; Sánchez-Herencia, J.A.; Bartolomé, J.F.; Tanimoto, T. Elastic modulus in rigid Al_2O_3/ZrO_2 ceramic laminates. *Scripta Materialia*, **1997**, *37, Issue 7*, 1095–1103, DOI: 10.1016/S1359-6462(97)00205-4
52. Baumann, A.; Mayer, D.; Moritz, T.; Lenk, R. Stahl-Keramik-Verbunde durch Pulverspritzgießen, in *Verbundwerkstoffe. 17. Symposium Verbundwerkstoffe und Werkstoffverbunde 2009*, Bayreuth, Krenkel, W., Weinheim: Wiley-VCH, 502-512
53. Zschippang, E.; Mannschatz, A.; Klemm, H.; Moritz, T.; Martin, H.-P. Charakterisierung und Verarbeitung von Si_3N_4-SiC-$MoSi_2$-Kompositen für Heizleiteranwendungen, *Keramische Zeitschrift*, **2013**, *05*, 294-297
54. Scheithauer, U.; Haderk, K.; Richter, H.-J.; Petasch, U.; Michaelis, A. Influence of the kind and amount of pore forming agents on the thermal shock behaviour of carbon-free refractory components produced by multilayer technology. *refractories WORLDFORUM*, **2011**, *4, Issue 1*, 130-136
55. Scheithauer, U.; Slawik, T.; Haderk, K.; Moritz, T.; Michaelis, A. Development of Planar and Cylindrical Refractories with Graded Microstructure. Proceedings of UNITECR 2013, 13th Biennial Worldwide Congress on Refractories, Victoria, Canada, 339-343
56. Scheithauer, U.; Schwarzer, E.; Otto, C.; Slawik, T.; Moritz, T.; Michaelis, A. Ceramic and metal-ceramic components with graded microstructure. 11th International Conference on Ceramic Materials and Components for Energy and Environmental Applications, Ceramic Transactions, 256, 2016

Preprints (www.preprints.org) | NOT PEER-REVIEWED | Posted: 10 October 2017 doi:10.20944/preprints201710.0057.v1

Peer-reviewed version available at Materials 2017, 10, 1368; doi:10.3390/ma10121368

57. Mannschatz, A.; Moritz, T.; Jegust, S.; von Witzleben, M. Enabling Co-Sintering of ATZ/ZTA Ceramic Compounds by Two-Component Injection Moulding with Green Tapes as Interlayers, proceedings of Euro PM2011 – Powder Injection Moulding - Advance Processing
58. Mannschatz, A.; Härtel, A.; Müller-Köhn, A.; Moritz, T.; Michaelis, A., Wilde, M.: Manufacturing of Two-colored Co-sintered Zirconia Components by Inmold-labelling and 2C-Injection Molding. *cfi/Ber. DKG*, **2014**, *91, No. 8*
59. Sand, C.; Adler, J.; Lenk, R. A new concept for manufacturing sintered materials with a three dimensional composition gradient using a silicon carbide - Titanium carbide composite, in: W.A. Kaysser (Ed.), Functionally Graded Materials 1998, Proceedings of the 5th International Symposium on FGM, Dresden, Germany, 26–29 October 1998, Trans Tech Publications, Switzerland, 1999, 65–70.
60. Hermel, W.; Adler, J.; Sand, C. Final Report, DFG-Programme 322733, Project Sintered Materials with a Three Dimensional Graded Composition and/or a Three Dimensional Graded Porosity, 2002.
61. Zhang, Y.; Han, J.; Zhang, X.; He, X.; Li, Z.; Du, S: Rapid prototyping and combustion synthesis of TiC/Ni functionally gradient materials, *Materials Science and Engineering: A*, **2001**, *299, Issues 1–2*, 218–224, DOI: 10.1016/S0921-5093(00)01377-0
62. Scheithauer, U.; Schwarzer, E.; Richter, H.J.; Moritz, T. Thermoplastic 3D Printing – An Additive Manufacturing Method for Producing Dense Ceramics. *JACT*, **2014**, *12 (1)*, 26-31, DOI: 10.1111/ijac.12306
63. Scheithauer, U.; Bergner, A.; Schwarzer, E.; Richter, H.-J.; Moritz, T. Studies on thermoplastic 3D printing of steel–zirconia composites. *J Mat Res*, **2014**, 29 (17), 1931 – 1940, DOI: 10.1557/jmr.2014.209
64. Scheithauer, U.; Slawik, T.; Schwarzer, E.; Richter, H.-J.; Moritz, T.; Michaelis, A. Additive Manufacturing of Metal-Ceramic-Composites by Thermoplastic 3D- Printing, *J. Ceram. Sci. Tech.*, **2015**, *06 [02]*, 125-132, DOI: 10.4416/JCST2014-00045
65. Scheithauer, U.; Schwarzer, E.; Haertel, A.; Richter, H.J.; Moritz, T.; Michaelis, A. Processing of thermoplastic suspensions for Additive Manufacturing of Ceramic- and Metal-Ceramic-Composites by Thermoplastic 3D-Printing (T3DP), 11th International Conference on Ceramic Materials and Components for Energy and Environmental Applications, Ceramic Transactions, 256, 2016
66. Scheithauer, U.; Pötschke, J.; Weingarten, S.; Schwarzer, E.; Vornberger, A.; Moritz, T.; Michaelis, A. Droplet-based additive manufacturing of hard metal components by thermoplastic 3D printing (T3DP), *Journal of Ceramic Science and Technology: An international Journal reporting on the synthesis, structure and properties of ceramics*, **2017**, *8 (1)*, 155-160, DOI: 10.4416/JCST2016-00104